Electrochemical Behavior of Mesoporous Tin Phosphate Anode upon Reaction with Lithium

S. M. Hasanaly[1]* and M. A. Bustam[2]

[1]Advance Materials Research Centre,
(AMREC), SIRIM Berhad,
Lot 34, Jalan Hi-Tech 2/3, Kulim Hi-Tech Park, 09000 Kulim, Kedah, Malaysia
[2]Department of Chemical Engineering,
Universiti Teknologi PETRONAS, 31750 Tronoh, Perak, Malaysia

*Corresponding author: munirah@sirim.my

Abstract: *The electrochemical behavior of mesoporous tin phosphate (SnP_2O_7) was studied for possible application as the anode material in lithium-ion batteries. This tin phosphate material which was prepared via a surfactant templating method and calcined at 400°C, showed an average pore size distribution of 18 nm. Cyclic voltammogram and differential capacity plot analyses indicated irreversible reduction of tin phosphate to lithium phosphate and tin upon initial reaction with lithium and subsequently followed by the reversible alloying and de-alloying reaction of lithium with tin. The mesoporous tin phosphate exhibited initial reversible capacity of 265 mAh/g and good capacity retention of 188 mAh/g upon reaching the 10th cycle.*

Keywords: mesoporous tin phosphate, anode material, charge-discharge, capacity, lithium-ion battery

1. INTRODUCTION

Much attention has been given to the potential of substituting tin-based materials for carbon negative electrodes in lithium-ion batteries. However, there are a few drawbacks that hinder the practical application of tin-based anode materials. The major deficiencies of this material are their significant irreversible capacity loss in the first cycle, poor cyclability and volume changes effects that lead to disintegration and loss of electronic and ionic contact.[1] The cause of capacity fading of tin oxide anode was elaborated by Courtney and Dahn[2,3] in a two-step reaction, as follows:

$$4Li^+ + 4e^- + SnO_2 \rightarrow 2Li_2O + Sn \quad (1)$$

$$Sn + xLi + xe^- \leftrightarrow Li_xSn \quad (0 \leq x \leq 4.4) \quad (2)$$

In the first step, tin oxide (SnO_2) reacts with lithium (Li) to form lithium oxide (Li_2O) and metallic tin (Sn) particles which are dispersed in the Li_2O oxide matrix. Although the formation of Li_2O in the first step is irreversible, it contributes to the mechanical integrity of the anode.[2,3] Further reaction of Sn with Li leads to the formation of Li-Sn alloy up to the composition of $SnLi_{4.4}$. The second step involves the reversible Li-Sn alloying and de-alloying process. Upon prolonged cycling Sn atoms aggregate and form larger Sn clusters which generate huge volume changes in the material that eventually led to the disintegration of this anode material.[2,3] Dahn's group[3,4] showed that the rate of tin aggregation and capacity fade can be decreased by incorporating spectator atoms such as boron (B) and phosphorus (P) in the Li_2O matrix. This can be explained based on the active-inactive mixed conductor matrix concept proposed by Huggins.[5] The active component in the electrochemical reaction with Li is Sn whereas the spectator atoms which create a matrix that holds the dispersed Sn particles, remains inactive. The inactive matrix holds the Sn particles together and retards its aggregation during the reversible reaction which in turn buffers volume expansion effects of the reactants.[3–5] The inactive matrix phase not only determines and maintains the structural integrity of the anode but also acts as a current collector and a medium that allows rapid transport of Li ions.[5] The use of a composite tin-based anode with an active and inactive phase has been reported to exhibit considerable improvement in the cycling performance of Li-ion cells.[3–7]

Mesoporous materials has been extensively investigated for application in catalysts, absorbents, sensors and optoelectronics and it is possible to extend its potential application as host material for Li-ion cells. Kim et al. first reported that mesoporous/crystalline tin phosphate (SnP_2O_7) composite exhibited reversible pore changes during reaction with Li.[8] Mesoporous materials have uniform pore structures, high specific surface area and specific pore volume. It is suggested that the interspaces in the mesoporous structure can accommodate the volume variations during cycling thus preserving the anode integrity.[9] Phosphate-based materials show promising potential as alternative anode host material as their layered structure provide sites that enable reversible Li insertion and extraction to take place at relatively low potential.[10,11]

In this study, a mesoporous tin phosphate was synthesised via a surfactant templating method with the expectation that the mesoporous structure can buffer the volume changes to some extent and result in better capacity retention ability.

2. EXPERIMENTAL

2.1 Synthesis and Characterisation of Mesostructured Tin Phosphate

An anionic surfactant, sodium dodecyl sulphate, SDS ($NaC_{12}H_{25}SO_4$, Fluka, Switzerland) was used as a templating surfactant and tin (IV) chloride ($SnCl_4$, 99%, Aldrich, USA) was selected as the starting tin source. An aqueous solution of $SnCl_4$ was added to 1M of SDS aqueous solution with continuous stirring at room temperature. Phosphoric acid (H_3PO_4, 86%, J. T. Baker, USA) was then slowly added into this mixture. The mixed solution gradually transformed into a block of whitish and very viscous gel. The gel was then loaded into a Teflon lined stainless steel vial which was then placed into a vacuum oven and aged at 100°C for 5 days. The resulting product was filtered, washed with purified water and dried at ambient temperature. Precursors were preheated at 200°C for 2 hours in air and then calcined at 300°C, 400°C and 500°C for 4 hours.

Thermogravimetric analysis (TGA) was conducted with a Netzsch Simultaneous Thermal Analyser (STA409C) in argon atmosphere. Powder x-ray diffraction (XRD, BRUKER Advance D-8 X-Ray Diffractometer, Germany) measurements using Cu K_α radiation were used to characterise the structures of the synthesised powders. Elemental compositions were analysed by inductively coupled plasma spectroscopy ICPS (Inductively Coupled Plasma Optical Emission Spectrometer, ICP-OES, Perkin Elmer Optima 2000DV, USA) using acid digestions of the tin phosphate powder. The synthesised powder calcined at 400°C was degassed overnight at 100°C for nitrogen adsorption-desorption isotherm measurement which was recorded with an adsorption apparatus from Quantachrome (Autosorb 1-C, Germany).

2.2 Electrochemical Characterisation

For electrochemical measurements, the electrode was prepared by mixing the tin phosphate powder (70% in weight) with a blend of acetylene black and polyvinylidene fluoride (PVDF) (30% in weight) in an agate mortar. Acetylene black was added to provide additional conductivity to the tin phosphate anode during electrochemical tests whereas PVDF merely acts as a binder in the anode preparation. This mixture was spread and pressed onto a stainless steel mesh. The electrode was then dried at ~120°C in an oven. Electrochemical test cell are assembled in an argon-filled glove box where 1M lithium hexafluorophosphate ($LiPF_6$) in a 1:2 mixture of ethylene carbonate:dimethyl carbonate (EC:DMC) was used as the electrolyte. Cyclic voltammetry measurement was carried out with the WonATech Battery Cycler System (WBCS3000, Korea), where Li foils

were used as reference and counter electrodes. The test cell was potentially scanned between 0–2V versus Li^+/Li at a rate of 0.100 mV/s. Charge and discharge performance tests was carried out at a constant current of 0.5 mA within the potential range of 0–1.5 V versus Li^+/Li with the WonATech Battery Cycler System.

3. RESULTS AND DISCUSSION

3.1 Structural Characterisation

The surfactant species is removed by calcination process. TGA of the as-synthesized tin phosphate sample revealed nearly 40% total weight loss upon heating to 400°C. These losses are attributed to the evaporation of moisture and decomposition of organic matter. Above 400°C, the weight of the sample hardly changes which indicates that the surfactant is completely removed from the tin phosphate around 400°C.

The XRD patterns of the tin phosphate powders calcined at 200°C, 300°C, 400°C and 500°C are shown in Figure 1. The diffraction pattern in $2\theta=20°–80°$ region for all the calcined tin phosphate samples shown in Figure 1(a), revealed no characteristics peaks. The intensities observed are generally weak suggesting that these materials are largely amorphous even when heated to 500°C. Mesostructure characteristics were analysed using the low angle XRD pattern at $2\theta°=1°–10°$, as shown in Figure 1(b). The presence of low angle reflections at around 1.5° for samples calcined at 200°, 300°C and 400°C indicates mesostructured material characteristics. Mesoscopic order of this tin phosphate powder was preserved upon removal of the surfactant by calcination at 400°C but when further calcined to 500°C, the mesoporous structure had collapsed. Mesoporous structure has been reported to collapse at high temperature.[12] It is therefore crucial to determine the appropriate calcination temperature that just removes the surfactant species to form a stable mesostructure.[12] In this work, the mesoporous tin phosphate is thermally stable at 400°C as indicated by TGA and XRD findings.

Due to the amorphous nature of the sample, it was difficult to determine the identity of the compound using the XRD technique. Elemental analysis was conducted using the ICPS. Measurements on the tin phosphate powder calcined at 400°C indicated molecular formulae of $Sn_{1.0}P_{1.96}O_{7.06}$. The oxygen contents were calculated from the difference between sample weights and the sum of the P and tin (Sn) contributions.

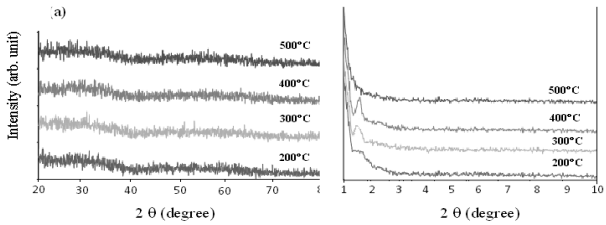

(a) (b)

Figure 1: XRD pattern of: a) tin phosphates calcined at different temperature within diffraction range of 2θ°=20°–80° and (b) tin phosphate calcined at different temperature within diffraction range of 2θ=1°–10°.

Nitrogen adsorption-desorption isotherm for the mesostructured tin phosphate calcined at 400°C is shown in Figure 2. The shape of this hysteresis is indicative of a mesoporous material with open slit-shaped pores.[13,14] The specific Brunauer-Emmett-Teller (BET) surface area of the particles is 110.13 m^2/g. Inset in Figure 2 shows an average pore size distribution of 18 nm as determined using the Barrett-Joyner-Halenda (BJH) model based on the desorption branch isotherm.

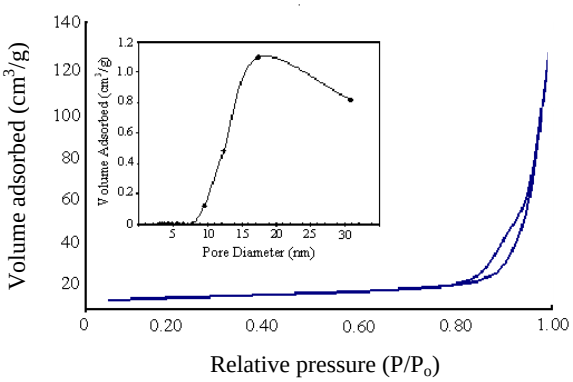

Figure 2: Nitrogen sorption isotherm of tin phosphate calcined at 400°C. Inset figure shows pore size distribution.

3.2 Electrochemical Characterisation

3.2.1 Cyclic voltammetry

Figure 3 shows the cyclic voltammogram of the mesoporous tin phosphate. The first scan begins cathodically from open circuit potential at 2.6 V down to 0 V. The voltammetric response of the first cycle is noticeably different

from the subsequent cycles. One large cathodic peak at around 1.2 V only appeared in the first scan cycle indicating that the reaction occurring at this point is irreversible. According to Courtney and Dahn[2,3], this large first cycle irreversible cathodic peak can be assigned to decomposition of tin phosphate upon initial reaction with Li. The decomposition products would be Sn particles dispersed in a lithium phosphate ($Li_4P_2O_7$) matrix. The next cathodic peak was found at around 0.18 V whereas upon the reverse anodic scan, a small peak was detected around 0.54 V. These peaks are visible in the second and third cycles. This pair of redox peaks is attributed to the reversible reaction of Li alloying and de-alloying with Sn.

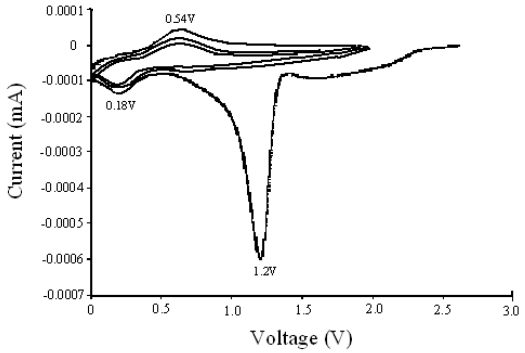

Figure 3: Cyclic voltammogram of mesoporous tin phosphate.

3.2.2 Charge and discharge profiles

Initial discharge (Li^+ insertion) and charge (Li^+ extraction) capacity profile for mesoporous tin phosphate is shown in Figure 4. Upon discharging to 0 V, a capacity of 1236 mAh/g was obtained. Subsequent charging up to 1.5 V, returned a reversible capacity of 265 mAh/g indicating a loss of 78% in irreversible capacity. This loss is caused by the irreversible reaction between Li and tin phosphate to form irreversible lithium phosphate phases and metallic Sn, which could then be used to store and release Li^+ reversibly. It has been suggested that electrolyte species decomposition on the anode surface may also add to the first cycle capacity loss.[15,16]

Figure 5 shows the differential capacity plot constructed from the initial charge discharge curve of mesoporous tin phosphate. The cathodic spike at potential around 1.19 V agrees well with the first cycle cathodic peak in the cyclic voltammogram in Figure 3, indicating the decomposition of mesoporous tin phosphate and formation of metallic Sn. The exact identity of the cathodic peak at around 0.7 V has yet to be confirmed but it is speculated to be attributed

to the formation of the irreversible lithium phosphate phase.[3,16] These two

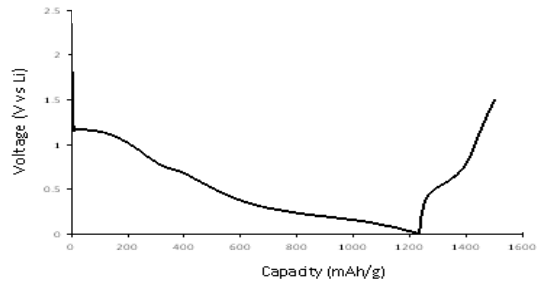

Figure 4: Initial charge discharge curve of mesoporous tin phosphate.

reactions are irreversible as the peaks are no longer visible in the differential capacity plot based of the second charge discharge curve as represented in Figure 6. Corresponding peaks at around 0.18 V and 0.58 V which could be detected from both Figures 5 and 6, represent Li insertion and extraction process which are responsible for the reversible reaction in the following cycles. This pair of peaks also corresponds well with the result obtained in Figure 3.

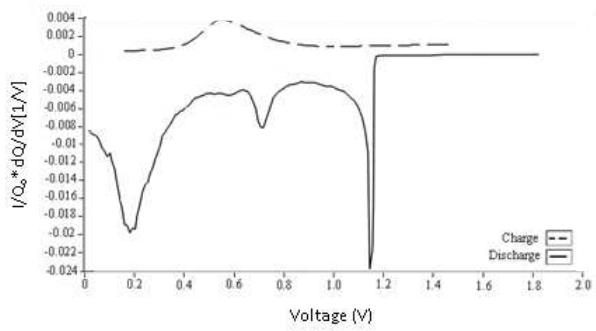

Figure 5: Differential capacity plot from initial charge discharge curve of mesoporous tin phosphate.

Capacity obtained from cycling mesoporous tin phosphate anode for 10 cycles is shown in Figure 7. From the second cycle, only a reversible capacity of 265 mAh/g was recovered from the initial discharge capacity of 1236 mAh/g. Upon reaching the 10th cycle, a reversible charge capacity of 188 mAh/g was retained. It is believed that huge volume expansion occurs during the initial discharging to form the irreversible phase that caused about 78% in irreversible capacity losses.

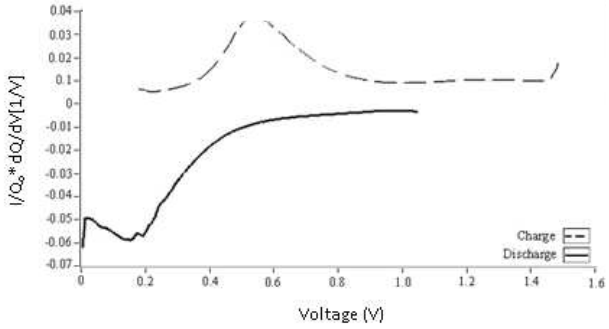

Figure 6: Differential capacity plot from second charge discharge curve of mesoporous tin phosphate.

Subsequent charging and discharging process result in only small volume changes effects. This may be attributed to the mesoporous framework which was able to dissipate most of the mechanical stress induced by volume changes during the Li-Sn alloying and de-alloying reactions through reversible pore expansion and contraction mechanism.[12] Capacity losses of 29% were observed upon reaching the 10th cycle. This is probably due to inevitable aggregation of Sn or Li-Sn clusters.[3] As these phases have different unit cell volumes, their repetitive expansion and contraction during charging and discharging process increases mechanical stresses which eventually lead to the electronic connectivity losses and capacity fading.[16]

3.2.3 Mechanism of lithium reaction with mesoporous tin phosphate

Attidekou et al.[17] have proposed a three step mechanism explaining the electrochemical reaction of Li with tin phosphate. The first reaction with Li results in the formation of lithium phosphate and metallic Sn. Further reaction with Li leads to the irreversible reduction of the $Li_4P_2O_7$ matrix to $Li_6P_2O_7$ and the reversible Li alloying with Sn to form $Li_{22}Sn_5$. These reactions are expressed as below;

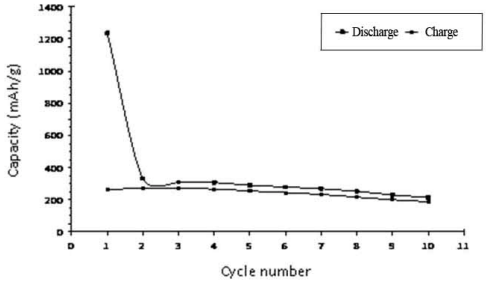

Figure 7: Capacity vs. cycle number plot of mesoporous tin phosphate.

$$4Li^+ + 4e^- + SnP_2O_7 \rightarrow Li_4P_2O_7 + Sn \quad (3)$$

$$2Li^+ + 2e^- + Li_4P_2O_7 \rightarrow Li_6P_2O_7 \quad (4)$$

$$xLi^+ + xe^- + Sn \leftrightarrow Li_xSn\ (0 \leq x \leq 4.4) \quad (5)$$

Experimental capacity loss of up to 971 mAh/g is mainly due to the reactions (3) and (4). Another possible cause that adds to the loss value is the reduction of electrolyte species to form passive films on the anode surface.[15,16] Reaction (5) which involves the alloying and de-alloying of Li-Sn is responsible for the rechargeability of the mesoporous tin phosphate anode.

This mesoporous tin phosphate has performed better in terms of capacity retention when compared to that of the non-porous, amorphous tin phosphate prepared by Lee et al.[16] Upon cycling to the 10th cycle, Lee's material retained a reversible capacity of 48% with 52% losses in capacity[16] whereas the mesoporous tin phosphate in this work retained a reversible capacity of 71% with 29% in capacity loss. The lower losses in capacity upon repeated cycling is attributed to the mesoporous structure. The mesopores provides larger surface area that permits better flooding of the electrolyte with the tin phosphate particles and this results in better transferring of Li^+ and electrons and enhance the cycling performance. The capacity loss from volume changes upon repeated cycling is also minimised as the mesopores provide space that suppresses volume expansion during Li^+ insertion thus avoiding the cracking of the anode material and maintaining better conduction pathway for the electrochemical reaction to occur.[18]

4. CONCLUSION

Amorphous tin phosphate was synthesized using SDS surfactant and tin (IV) chloride and was further calcined to 400°C to remove residual surfactant in order to obtain the mesoporous structure. Initial reaction of mesoporous tin phosphate anode with Li results in the reduction of tin phosphate to Sn, lithium phosphate and $Li_6P_2O_7$ matrixes. This initial reaction which is irreversible is responsible for the huge capacity losses of about 78% in the first cycle. The reversible reaction of alloying and de-alloying of Li_xSn ($0 \leq x \leq 4.4$) compound upon further charging and discharging cycles is the basis of rechargeability for mesoporous tin phosphate anodes. The mesoporous tin phosphate anode was able to retain a reversible capacity of 188 mAh/g upon reaching the 10th cycle with a capacity loss of 29%. The mesoporous structure of tin phosphate provides channels that facilitates the Li^+ insertion and extraction and contributes significantly to the improved capacity retention by accommodating the volume changes during cycling.

5. REFERENCES

1. Winter, M. & Besenhard, J. O. (1999). Electrochemical lithiation of tin and tin-based intermetallics and composites. *Electrochim. Acta,* 45(1–2), 31–50.
2. Courney, I. A. & Dahn, J. (1997). Electrochemical and in-situ x-ray diffraction studies of the reaction of lithium with tin oxide composites. *J. Electrochem. Soc.,* 144(6), 2045–2052.
3. Courney, I. A. & Dahn, J. (1997). Key factors controlling the reversibility of the reaction of lithium with SnO_2 and Sn_2BPO_6 glass. *J. Electrochem. Soc.,* 144(9), 2943–2948.
4. Courney, I. A., McKinnon, W. R. & Dahn, J. (1999). On the aggregation of tin in SnO composite glasses caused by the reversible reaction with lithium. *J. Electrochem. Soc.,* 146(1), 59–68.
5. Boukamp, B. A., Lesh G. C. & Huggins, R. A. (1981). All solid lithium electrodes with mixed conductor matrix. *J. Electrochem. Soc.,* 128(4), 725–729.
6. Mao, O., Dunlap, R. A. & Dahn, J. R. (1999). Mechanically alloyed Sn-Fe(-C) powders as anode materials for Li-ion battery. *J. Electrochem. Soc.,* 146(2), 405–422.
7. Yang, J., Winter, M. & Besenhard, J. O. (1996). Small particle size multiphase Li-alloy anodes for lithium-ion batteries. *Solid State Ionics,* 90(1–4), 281–287.
8. Kim, E., Son, D. Y., Kim, T. G., Cho, J., Park, B. W., Ryu, K. S. & Chang, S. H. (2004). A mesoporous/crystalline composite material containing tin phosphate for use as anode in the lithium-ion batteries. *Angew. Chem. Int. Ed.,* 43, 5987–5990.
9. Harris, S. J., Despande, R. D., Que, Y., Dutta, I. & Cheng, Y. T. (2010). Mesopores inside electrode particles can change the Li-ion transport mechanism and diffusion-induced stress. *J. Mater. Res.,* 25(8), 1433–1440.
10. Behm, M. & Irvine, J. T. S. (2002). Influence of structure and composition upon performance of tin phosphate based negative electrodes for lithium batteries. *Electrochim. Acta,* 47(11), 1727–1738.
11. Moubtassim, E. M. L., Corredor, J. I., Tirado, J. L. & Vicente, P. C. (2001). $SnHPO_4$: A promising precursor for active material as negative electrode in Li-ion cells. *Electrochim. Acta,* 47(3), 489–493.
12. Yang, P. D., Zhao, D. Y., Margolese, D. I., Chmelka, B. F & Stucky, G. D. (1999). Block copolymer syntheses of mesoporous metal oxides with large ordering lengths and semicrystalline framework. *Chem. Mater.,* 11(10), 2813–2826.
13. Schneider, P. (1995). Adsorption isotherms of microporous-mesoporous solids revisited. *Appl. Catalysis A: General,* 129(2), 157–165.

14. Kruk, M. & Jaroniec, M. (2001). Gas adsorption characterization of ordered organic-inorganic nanocomposite materials. *Chem. Mater.*, 13(10), 3169–3183.
15. Li, J., Li, H., Wang, Z., Huang, X. & Chen, L. (1999). The interaction between SnO anode and electrolytes. *J. Power Sources*, 81–82, 346–351.
16. Lee, J. Y., Xiao, Y. W. & Liu, Z. L. (2000). Amorphous $Sn_2P_2O_7$, $Sn_2B_2O_5$ and Sn_2BPO_6 anodes for lithium ion batteries. *Solid State Ionics*, 133(1–2), 25–35.
17. Attidekou, P. S., Connor, P. A., Wormald, P., Tunstall, D. P., Francis, S. M. & Irvine, J. T. S. (2004). Solid state NMR studies of phosphate/tin matrix formed on electrochemical insertion into SnP_2O_7. *Solid State Ionics*, 175(1–4), 185–190.
18. Yin, X. M., Chen, L. B., Li, C. C., Hao, Q. Y., Li, Q. H., Zhang, E. D. & Wang T. H. (2011). Synthesis of mesoporous SnO_2 spheres via self-assembly and superior lithium storage properties. *Electrochim. Acta*, 56, 2358–2363.